Regional Cooperation for Limited Area Modeling in Central Europe

LACE nwp central europe

Data assimilation of all-sky radiance observations from MTG IRS II

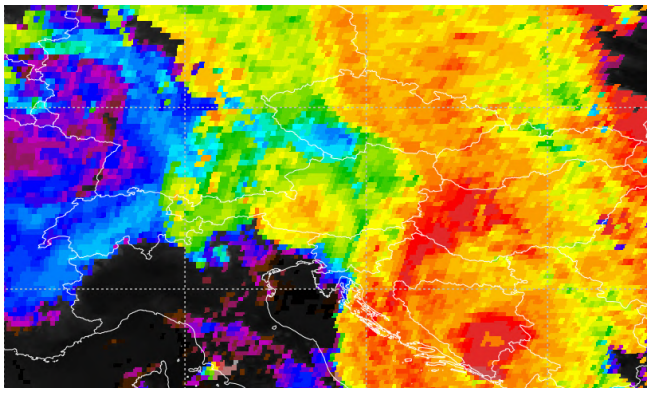

Author: Suzana Panežić (DHMZ)

Supervisors: Benedikt Strajnar (ARSO), Florian Meier and Adhithiyan Neduncheran (GeoSphere Austria)

Place: ARSO, Ljubljana and GeoSphere Austria, Vienna

Dates: 27th January - 7th February 2025. and 23nd June - 4th July 2025.

GeoSphere Austria · DHMZ · Czech Hydrometeorological Institute · HungaroMet · IMGW · Meteo Romania · SHMU · ARSO Meteo Slovenia

1 Introduction

The InfraRed Sounder (IRS) aboard the Meteosat Third Generation (MTG) satellite was launched on July 1st 2025 and is currently in its commissioning phase. Operational distribution of IRS data is expected by the end of 2026 (latest information from EUMETSAT).

To fully exploit the potential of high-resolution IRS radiance data in numerical weather prediction (NWP) systems, a robust all-sky data assimilation framework is required. As a first step toward this goal, work began in the previous year on the technical implementation of an all-sky system using IASI observations as a proxy [1]. At that stage, only a basic all-sky assimilation capability was implemented in the AROME model, relying on a simplified (dummy) inflation of observation errors for cloud-affected data.

The primary objective of this study is to extend this initial framework and implement a physically motivated, dynamically varying observation error model for selected water vapour channels. Specifically, following the work of Okamoto [2], the aims are to:

- fully implement and calibrate cloud-dependent observation error modelling;
- investigate additional quality control procedures for strongly cloud-affected radiances;
- implement an additional cloud-dependent VARBC predictor;
- assess the impact of individual all-sky data assimilation components using the 3D-EnVar configuration of the C-LAEF AlpeAdria system.

2 Model setup specification

The experiments are performed using the C-LAEF (Convection-permitting Limited-Area Ensemble Forecasting) AlpeAdria system, formerly known as C-LAEF 1k. The main characteristics of the model configuration are summarized below.

- Model: AROME CY46T1 (16 members) + AROME CY48T3 (1 member)
- Domain: C-LAEF AlpeAdria; $\Delta x = 1$ km; 1500x1350 GP; 90 vertical levels,
- Coupling: 3h space consistent coupling from IFS
- Upper air analysis: 3D-Var (16 members) or EnVar scheme (1 member) using OOPS framework; 3h Assimilation cycle; REDNMC=0.5, Ensemble data assimilation B matrix;

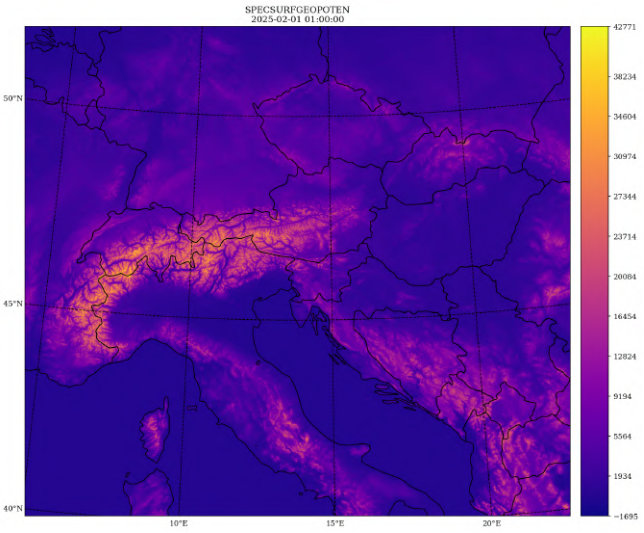

Figure 1: C-LAEF Alpe Adria domain

2.1 IASI data assimilation setup

The all-sky assimilation experiments focus on a limited number of water vapour sensitive IASI channels. The configuration is as follows:

- Channels assimilated in all-sky mode: 2951, 2958, 3049 and 3105
- Thinning distance: 10 km

These channels were selected due to their sensitivity to upper- and mid-tropospheric humidity and their relevance for cloud-affected radiance assimilation. All diagnostics within this report was performed using IASI data from a one month period: January 15th - February 15th 2025.

3 Code modification

To enable channel-dependent observation error modelling for all-sky infrared radiances, several modifications were introduced to the CY48T3_bf03 code. These changes build upon the developments implemented in the previous year and were complemented by merging the local development branch with the SEVIRI all-sky modifications provided by Adhithiyan Neduncheran [3].

All code changes are available at:

`https://github.com/spanezic/IAL/tree/CY48T3_bf.03_spanezic_IRallsky`

For reference, differences with respect to the clean CY48T3_bf03 export version can be found at:

`https://github.com/ACCORD-NWP/IAL/compare/CY48T3_bf.03...spanezic:IAL:CY48T3_bf.03_spanezic_IRallsky`

Routine: arpifs/module/yomsats.F90

Given the large number of channels provided by hyperspectral sounders, extending the existing SATGRP_TABLE with additional channel-specific parameters was deemed impractical. Instead, a new auxiliary table, SATOBERR_TABLE, was introduced. This table stores all variables required for all-sky observation error modelling. The SATOBERR_TABLE is allocated only when all-sky data assimilation is activated via the NAMSATS namelist and only for the subset of channels assimilated in all-sky mode. Although only a limited number of its fields are currently used, the table structure closely follows that of the microwave all-sky framework (agreement with the MF).

The table is populated from a new external namelist containing observation error related parameters for the selected channels. An example of the namelist content is shown below:

```
     ocean<-Tot Err(K)->land FG Err(K) ocean<-Cld amount->land alpha beta Clr
Channel Clr  Cldy Clr  Cldy Clr Clr  Cldy Clr  Cldy sea land sea land     Sky
2951    0.79 6.16 0.57 4.67 0   0.13 4.55 0.01 6.50 1   1    0   0    F   0
2958    0.79 6.16 0.56 4.66 0   0.13 4.55 0.01 6.00 1   1    0   0    F   0
3049    0.79 6.16 0.55 4.51 0   0.13 4.55 0.01 6.50 1   1    0   0    F   0
3105    0.79 6.16 0.56 3.51 0   0.13 4.55 0.01 5.97 1   1    0   0    F   0
proxy a def
2.0 2.0
```

Routine: arpifs/obs_preproc/allskyir_read_sat_error.F90

At ECMWF, the routine **arpifs/obs_preproc/read_iasichans.F90** is used to define all-sky IASI channels through a channel mask, with a constant observation error of 5.0 applied to cloud-affected observations. In order to avoid maintaining two separate namelists, this mask-reading mechanism was retained under an ECMWF logical switch.

A new routine was implemented to read the external all-sky observation error namelist. This routine populates both the SATOBERR_TABLE and the all-sky channel mask structure LALLSKY_IASI_BACK. The content of a standard SATGRP_TABLE is used in order to construct the name of the new external namelist. Since IASI data from Metop-B and Metop-C are used, two separate namelists are defined (content example in the previous subsection):

```
allskyir_error_metop_1_iasi.dat
allskyir_error_metop_3_iasi.dat
```

Routine: arpifs/obs_preproc/allskyir_setup.F90

A new routine to set up and initialize the all-sky IR framework described in the previous subsection. It's called from the **arpifs/var/rtsetup.F90**.

4 Modeling of the observation error

Routine: arpifs/op_obs/hretr_rad.F90

The observation error model described by Okamoto (2023) was implemented within the ECMWF IASI all-sky section of the routine. Within IFS, cloud-affected IASI observations are assigned a constant observation error of 5.0. This behaviour was preserved under an ECMWF logical switch. The Okamoto based observation error modeling:

```
ELSE
    ITER(1)=0
    ITER=FINDLOC(SATOBERR_TABLE(YDSET%GROUP)%ICH_NUM, VALUE=ICHAN, DIM=1)
    IF (ITER(1)>0) THEN
        !Cloud effect averaged
        ZCLDA=(ABS(ZTBTOT(JOBS,ICOUNT(JOBS))-ZTBCLR(JOBS,ICOUNT(JOBS))) &
        & +ABS(ZOBS(JOBS,ICOUNT(JOBS))-ZTBCLR(JOBS,ICOUNT(JOBS))))/2.0_JPRB

        !Obs error calculation for all-sky channels
        ZSDMIN=SATOBERR_TABLE(YDSET%GROUP)%RTOT_ERR_SI_CLR(ITER(1))
        ZSDMAX=SATOBERR_TABLE(YDSET%GROUP)%RTOT_ERR_SI_CLD(ITER(1))
        ZCAMIN=SATOBERR_TABLE(YDSET%GROUP)%SI_CLR(ITER(1))
        ZCAMAX=SATOBERR_TABLE(YDSET%GROUP)%SI_CLD(ITER(1))
        IF (ZCLDA <= ZCAMIN) THEN
            ZCLDOBSERROR=ZSDMIN
        ELSEIF (ZCLDA >= ZCAMAX) THEN
            ZCLDOBSERROR=ZSDMAX
        ELSE
```

```
            ZCLDOBSERROR = ZSDMIN + (((ZSDMAX-ZSDMIN)/(ZCAMAX-ZCAMIN))*(ZCLDA-ZCAMIN))
        ENDIF
        ROBODY%ERRSTAT%OBS_ERROR(IBODY) = ZCLDOBSERROR
        ROBODY%ERRSTAT%FINAL_OBS_ERROR(IBODY) = ZCLDOBSERROR
    ENDIF !ITER
ENDIF !LECMWF
```

The observation error standard deviation is computed as a piecewise linear function of an average cloud effect parameter. For each assimilated observation, routine computes the average cloud effect as the average of the absolute differences between total and clear-sky simulated brightness temperatures, and between observations and clear-sky simulations:

$$C_A = \frac{|B - B_{CLR}| + |O - B_{CLR}|}{2}$$

Based on the averaged cloud effect value, the observation error is interpolated between predefined minimum (clr; clear-sky) and maximum (cld; cloud-affected) standard deviation and average cloud effect values (which are retrieved from the SATOBERR_TABLE):

$$O_{err} = \frac{\sigma_{cld} - \sigma_{clr}}{C_{cld} - C_{clr}}(C_A - C_{clr})$$

This approach allows a smooth transition between clear-sky and cloudy conditions, avoiding abrupt changes in observation error [Figure 2].

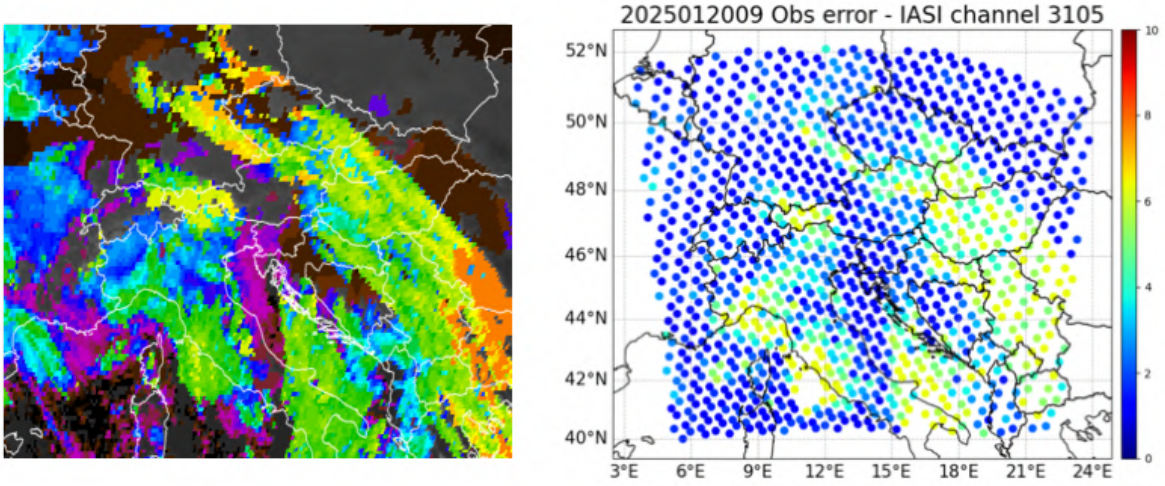

Figure 2: Eumetview: Cloud top product (left); Observation error values (right); January 20th 2025. 09 UTC

Figure 3 illustrates the derivation of the observation error parameters from the statistics of first-guess departures. Data are binned according to the averaged cloud effect, and the standard deviation within each bin is calculated. Typically, the standard deviation increases with averaged cloud effect up to a threshold, beyond which it remains approximately constant. A piecewise linear fit is then applied to define the minimum and maximum error values used in the assimilation.

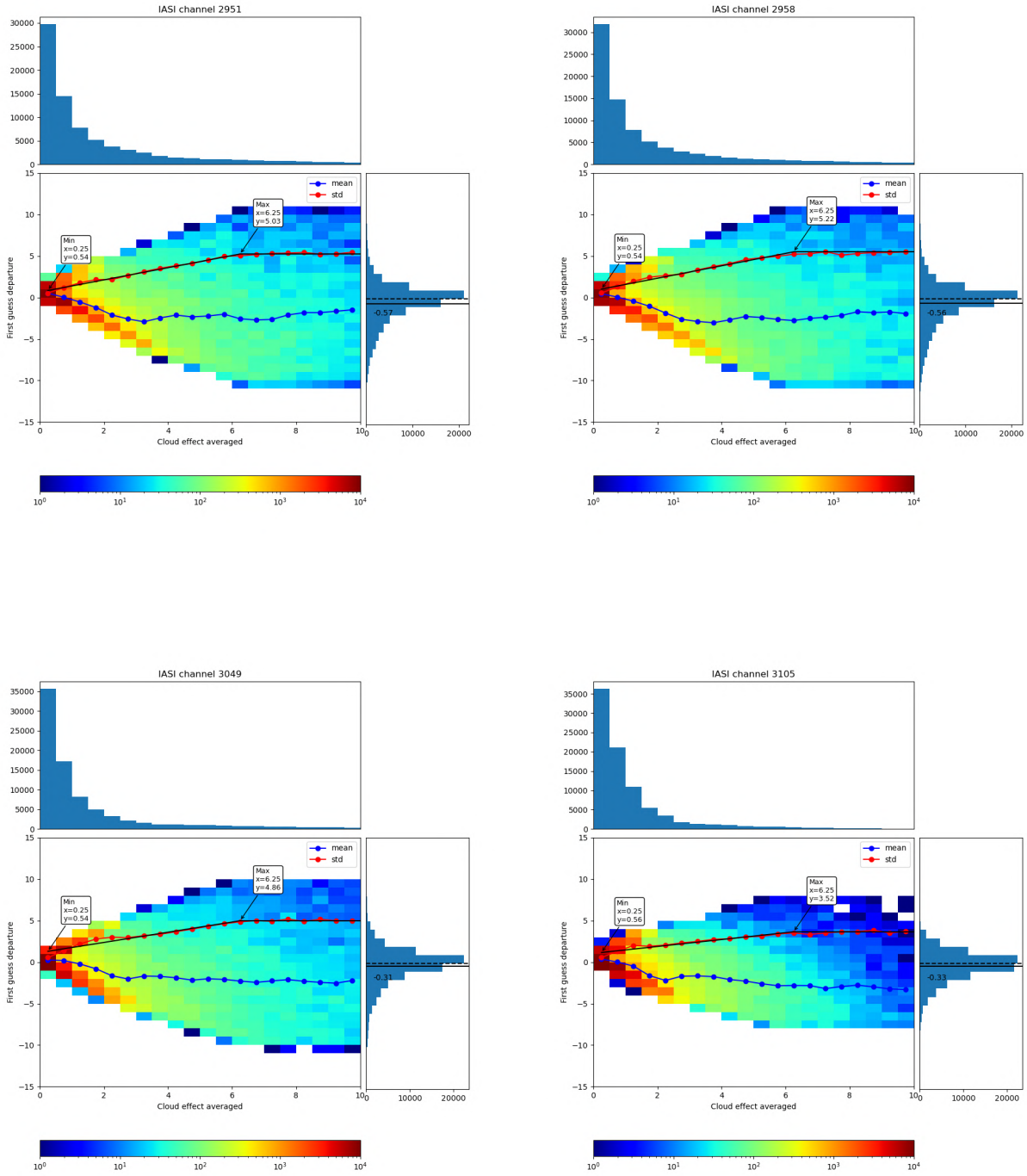

Figure 3: 2D histogram of first guess departures as a function of the averaged cloud effect; standard deviation (red marked line); bias (blue marked line); piecewise linear fit to standard deviation function (black line); minimum and maximum values marked within boxes; IASI channels 2951, 2958, 3049 and 3105

5 Rejection of strongly cloud-affected data

Radiance observations with an averaged cloud effect larger than 5 K represent strongly cloud-affected scenes, in which the simulated and/or observed brightness temperatures differ substantially from their clear-sky values. In the presence of thick, optically opaque clouds, the infrared signal cannot penetrate the cloud layer, and the measured radiance originates mainly from the cloud top. As a result, these observations contain little information about the underlying atmospheric temperature and humidity structure and cannot reliably constrain the analysis.

As part of the data quality control procedure, rejection of such data and their impact on the analysis will be explored. Relevant code modification is applied within the observation error modeling part of the **arpifs/op_obs/hretr_rad.F90** routine:

```
IF (ZCLDA > 5.0_JPRB) THEN
  ROBODY%BODY%DATUM_STATUS(IBODY) = ZCHSTAT_REJECT(ROBODY%BODY%DATUM_STATUS(IBODY)
ENDIF
```

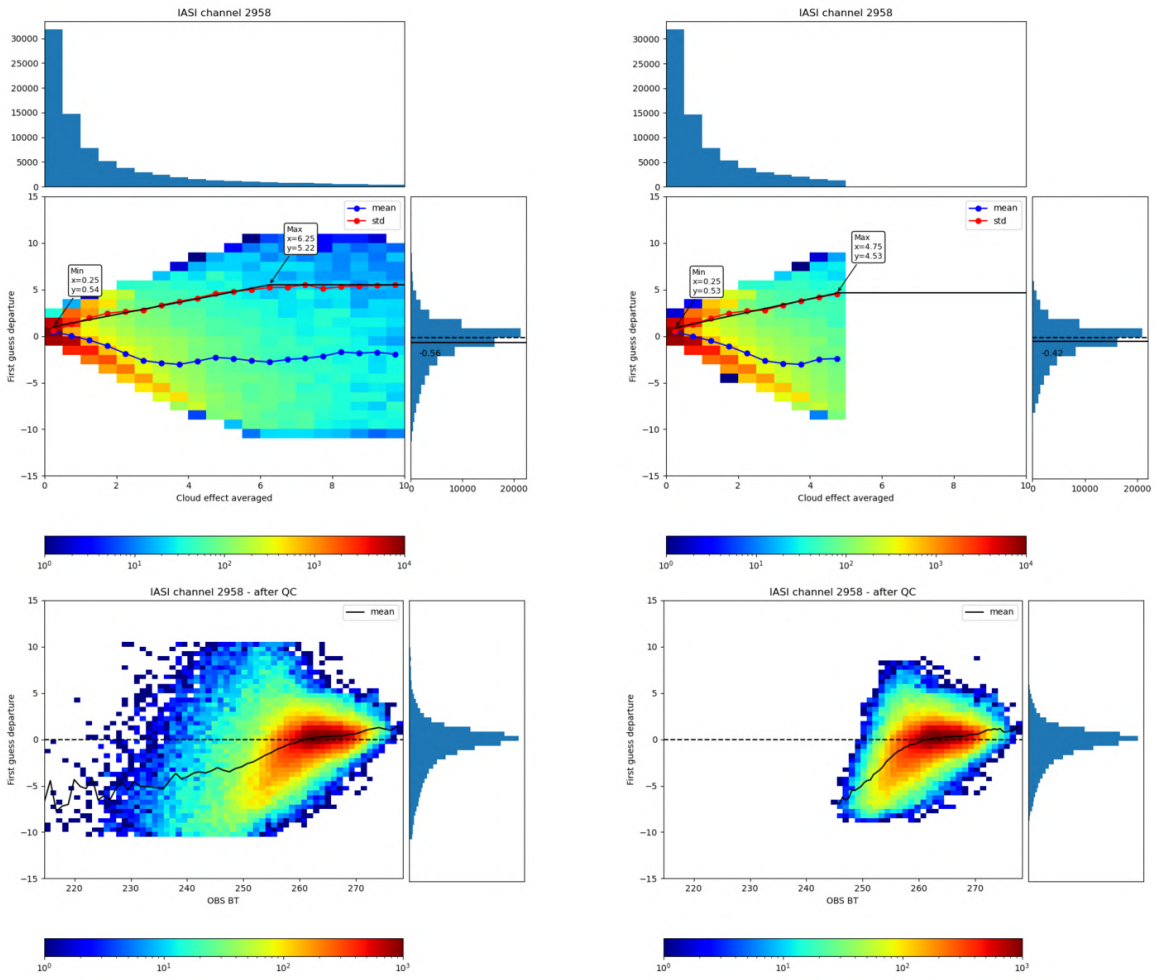

Figure 4: 2D histograms of first-guess departures as a function of averaged cloud effect (upper pictures) and observed brightness temperatures (lower pictures); With no rejection of strongly cloud-affected data (left); With rejection of strongly cloud-affected data (right)

Figure 4 shows the impact of rejecting strongly cloud-affected data on the first-guess departure distribution. After rejection, the distributions become more Gaussian and show a smaller spread.

6 Rejection of poorly simulated data

In a data assimilation system, observations are compared with their model-equivalent values. Observations that the model is unable to simulate realistically can introduce large errors and should therefore be rejected. To identify such cases, IASI window channel 1911 is used.

This channel is characterized by negligible gas absorption and a strong sensitivity to clouds. As a result, its radiances are primarily influenced by cloud properties rather than by atmospheric temperature or humidity. Channel 1911 is therefore well suited for diagnosing deficiencies in the model's representation of clouds and for identifying observations that are poorly simulated by the model.

This can be assessed by plotting the number of data points as a function of brightness temperature for both the observations and the model. For the model, total brightness temperature values (TBTOT) simulated by RTTOV are used.

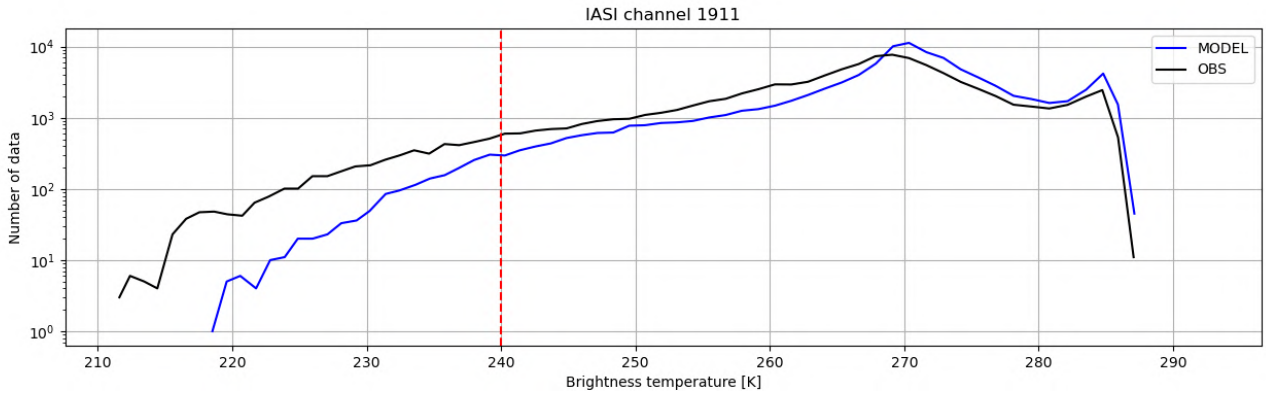

Figure 5: IASI channel 1911: number of data points as a function of brightness temperature for the observations (black line) and the model (blue line); Rejection threshold (red dashed line)

Figure 5 shows that the model exhibits a general lack of clouds compared to the observations. This is evident from the systematic differences between the model and observation distributions in the temperature range between 240 and 268 K. In addition, the model shows a larger number of clear-sky scenes, as indicated by discrepancies between 268 and 286 K. For brightness temperatures below 240 K, the divergence between the two distributions becomes more pronounced, indicating that the model struggles to represent very cold cloud tops, typically associated with high ice clouds. Consequently, observations with brightness temperatures below 240 K should be rejected, as they are poorly simulated by the model. This has also been implemented within the observation error modeling part of the **arpifs/op_obs/hretr_rad.F90** routine:

```
IF (ROBODY%BODY%OBSVALUE(IBODY) < 240.0_JPRB) THEN
    ROBODY%BODY%DATUM_STATUS(IBODY) = ZCHSTAT_REJECT(ROBODY%BODY%DATUM_STATUS(IBODY))
ENDIF
```

7 Impact studies

In order to assess the impact of the different all-sky data assimilation components, a set of experiments was performed using a one-month cycling period from January 15th to February 15th 2025. This extended period was necessary to accumulate a sufficient amount of IASI observations, as IASI data are available over Europe only twice per day.

Two reference experiments have been set up for the comparison:

- ref_clrsky - clear-sky IASI data assimilation
- ref_allsky - all-sky IASI data assimilation, no additional quality control

Two experiments with quality control applied:

- QC_CA - same as ref_allsky but with rejection of strongly cloud-affected data ($C_A > 5.0$)
- QC_CA_BT240 - same as QC_CA but with rejection of poorly simulated data ($T_b < 240K$)

The 3D-EnVar member of C-LAEF AlpeAdria system is used for all evaluations, without extending the control vector.

In order to evaluate the impact of different all-sky components in the assimilation of IASI data, ODB content was explored. In particular, their influence on other types of assimilated observations, such as radiosondes and AIREP reports, was assessed. These observations provide valuable information across the full vertical profile of the atmosphere and are therefore well-suited for quantifying the impact of all-sky IASI assimilation on the model background state.

In Figure 6, it can be seen that applying IASI quality control allows significantly more geopotential radiosonde data to pass without degrading the overall statistics. In fact, reductions in RMSE and bias are observed throughout almost the entire vertical profile. The increase in active radiosonde observations indicates that the background model state has moved closer to reality, particularly in the upper atmosphere (above 100 hPa). In contrast, when compared to the clear-sky experiment, the all-sky reference experiment without quality control shows a deterioration of the background model state near the surface, with large increases in RMSE and bias of radiosonde data, and in the upper atmosphere, where no radiosonde data pass quality control.

Figure 7 shows a similar increase in temperature radiosonde data passing quality control when IASI quality control is applied. The model state in the upper atmosphere (above 100 hPa) experiences cooling that aligns more closely with actual measurements, which allows more radiosonde data to pass. A notable difference from the geopotential case is that, for temperature, no significant RMSE or bias degradation occurs when IASI quality control is not applied. However, if observations with $T_b < 240K$ are not rejected, the negative increments meant for the upper atmosphere can be incorrectly projected to lower levels, which can degrade near-surface temperatures. This behaviour extends to specific humidity radiosonde and AIREP temperature data as can be seen in Figure 8 and Figure 9.

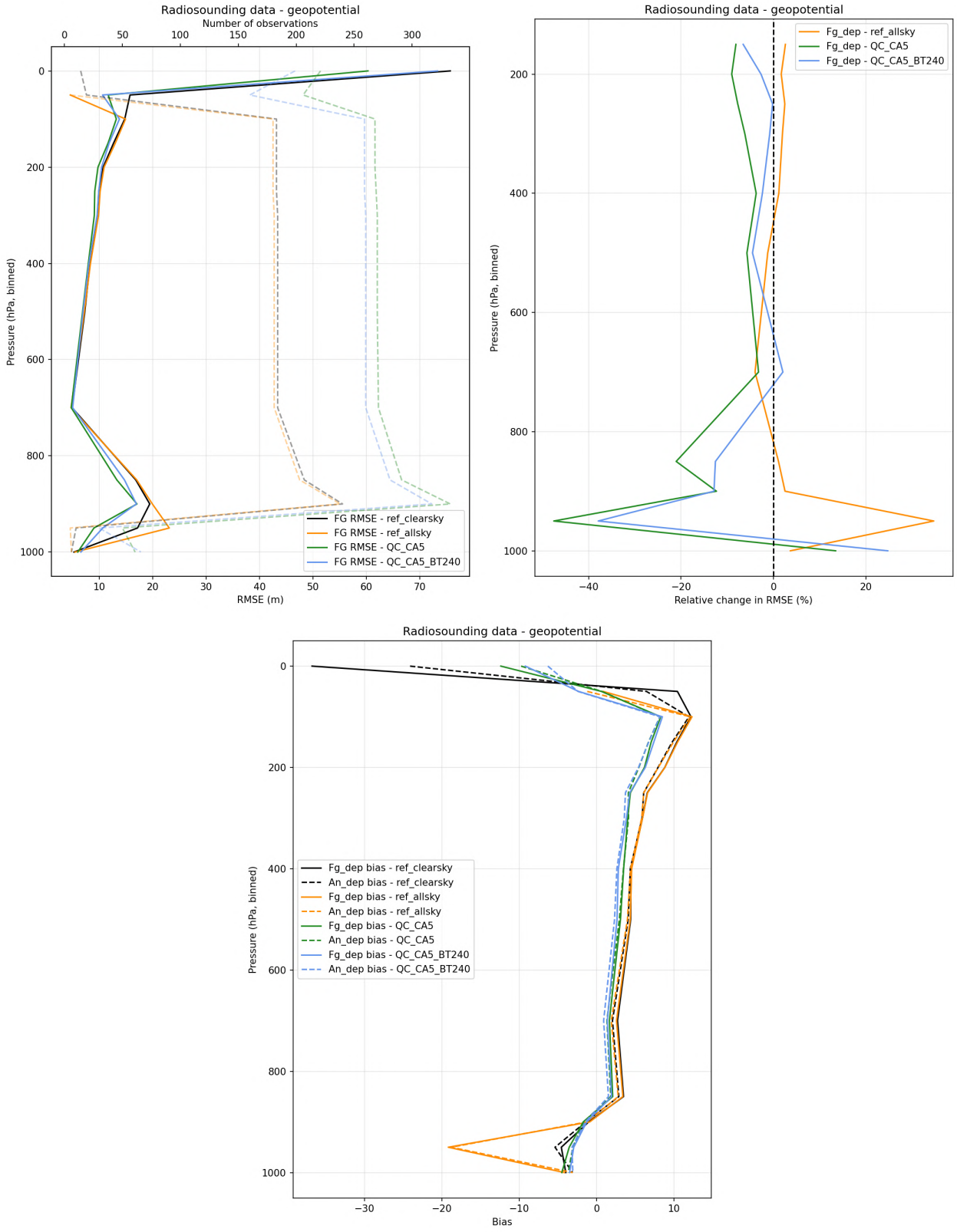

Figure 6: Radiosounding data - geopotential: averaged (binned by 50 hPa) vertical profile of RMSE (upper left); averaged relative change in vertical profile of RMSE when compared to clear-sky experiment (upper right); averaged vertical profile of bias (lower picture); ref_clrsky (black), ref_allsky (orange), QC_CA (green), QC_CA_BT240 (blue); transparent lines - number of data

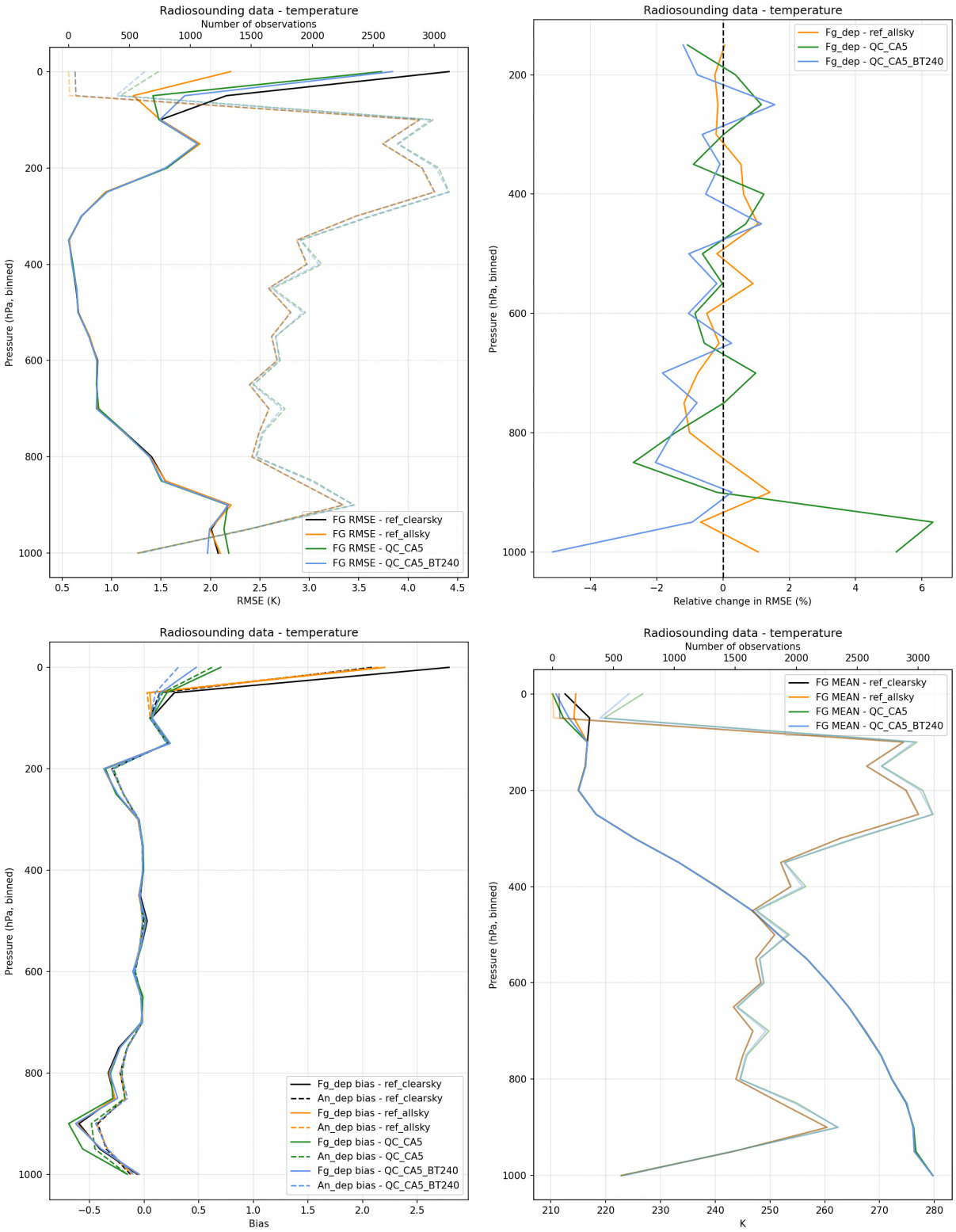

Figure 7: Radiosounding data - temperature: averaged (binned by 50 hPa) vertical profile of RMSE (upper left); averaged relative change in vertical profile of RMSE when compared to clear-sky experiment (upper right); averaged vertical profile of bias (lower left); averaged analysis temperature (lower right); ref_clrsky (black), ref_allsky (orange), QC_CA (green), QC_CA_BT240 (blue); transparent lines - number of data

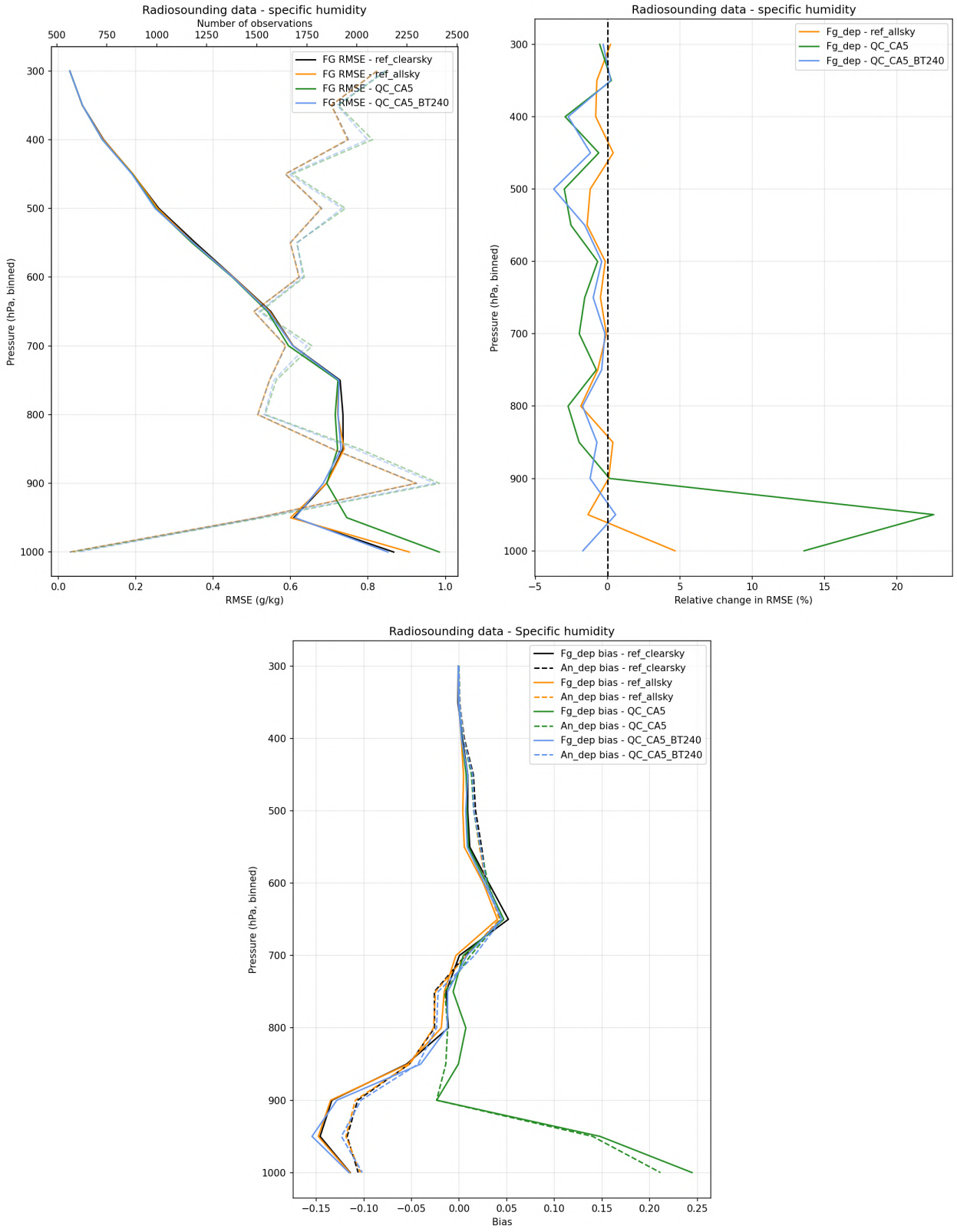

Figure 8: Radiosounding data - specific humidity: averaged (binned by 50 hPa) vertical profile of RMSE (upper left); averaged relative change in vertical profile of RMSE when compared to clear-sky experiment (upper right); averaged vertical profile of bias (lower picture); ref_clrsky (black), ref_allsky (orange), QC_CA (green), QC_CA_BT240 (blue); transparent lines - number of data

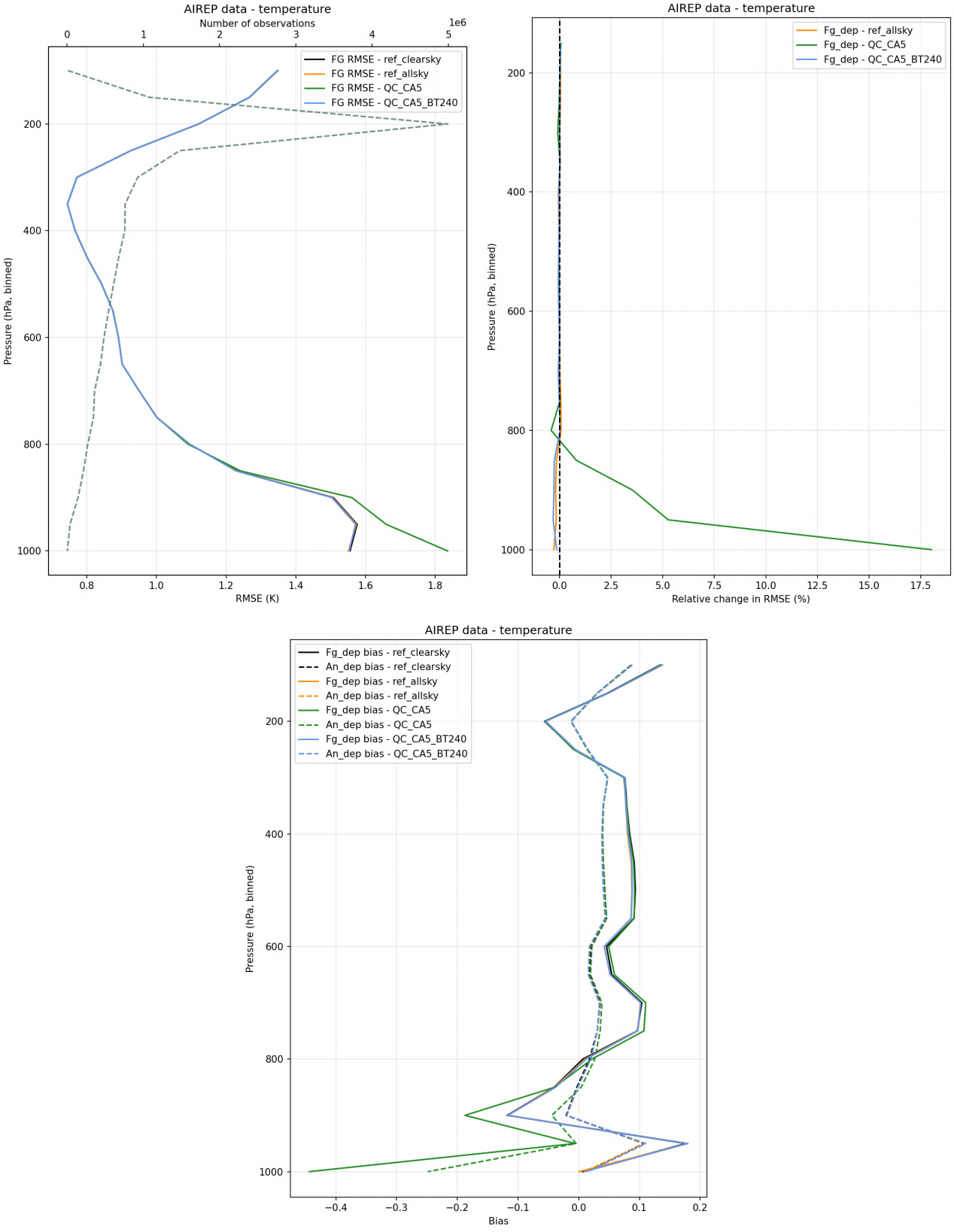

Figure 9: AIREP data - temperature: averaged (binned by 50 hPa) vertical profile of RMSE (upper left); averaged relative change in vertical profile of RMSE when compared to clear-sky experiment (upper right); averaged vertical profile of bias (lower left); averaged analysis temperature (lower right); ref_clrsky (black), ref_allsky (orange), QC_CA (green), QC_CA_BT240 (blue)

8 Averaged cloud effect as an additional VARBC predictor

Although the model background state shows overall improvement, the analysis indicates that a residual bias remains unresolved (Figure 10). In numerical weather prediction systems, satellite observations are corrected using an adaptive variational bias correction (VARBC) scheme [4]. To address the remaining residual bias, an additional cloud-dependent VARBC predictor is introduced, namely the averaged cloud effect (C_A).

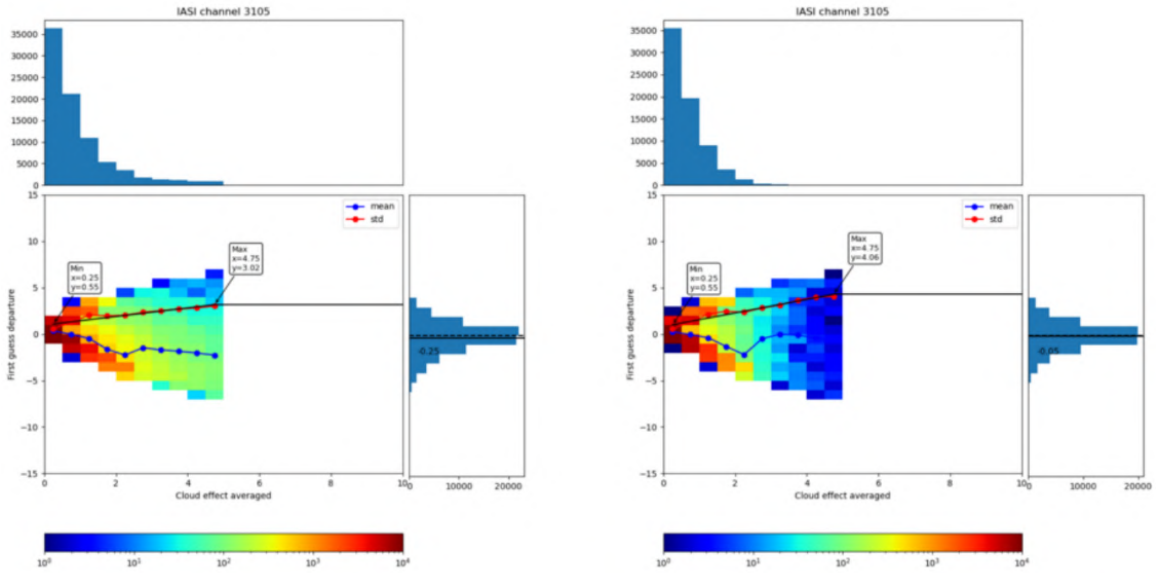

Figure 10: 2D histograms of first-guess departures as a function of averaged cloud effect; With rejection of strongly cloud-affected data (left); With rejection of strongly cloud-affected and poorly simulated data (right); standard deviation (red marked line); bias (blue marked line); piecewise linear fit to standard deviation function (black line); minimum and maximum values marked within boxes; IASI channel 3105

Routine: arpifs/module/varbc_pred.F90

This routine contains the VARBC predictor setup. In order to add an additional predictor, number of predictors is extended to 41, mapping it to a 8th place of observation related predictors. Description and normalization variables are extended, as well as pointers and default values related to the new predictor.

Changes made to this routine:

```
! Predictor information:
! ----------------------
! jpmxnpred predictors are indexed from 0 to jpmxnpred

INTEGER(KIND=JPIM), PARAMETER :: JPMXNPRED = 41
INTEGER(KIND=JPIM), PARAMETER :: JPMXNPARAM = JPMXNPRED+1
INTEGER(KIND=JPIM), PARAMETER :: JPMXBODYPRED = 7
INTEGER(KIND=JPIM), PARAMETER :: JBODYPREDSTART = 30
```

```
INTEGER(KIND=JPIM), PARAMETER :: JPREDNAME = 21
...
TYPE TYPE_VARBC_PRED
  INTEGER(KIND=JPIM) :: NVANG = 1
  INTEGER(KIND=JPIM) :: SOLZEANG = 2
  INTEGER(KIND=JPIM) :: DPDT = 3
  INTEGER(KIND=JPIM) :: PREC_FG = 4
  INTEGER(KIND=JPIM) :: PREC_OB = 5
  INTEGER(KIND=JPIM) :: VA = 6
  INTEGER(KIND=JPIM) :: DA = 7
  INTEGER(KIND=JPIM) :: CA = 8

  INTEGER(KIND=JPIM) :: IMAP(8)=(/-1,-1,-1,-1,-1,-1,-1,-1/)
  LOGICAL            :: LMAP(8)=(/.FALSE.,.FALSE.,.FALSE.,.FALSE.,.FALSE., &
  & .FALSE.,.FALSE.,.FALSE./)
...
CDPREDDESC(0:JPMXNPRED) = &
...
 &    'avr cloud effect     '/)
...
PPREDNORM(1:2,0:JPMXNPRED) = &
...
&        0.0_JPRB,     1.0_JPRB/),
...
REAL(KIND=JPRB), POINTER :: ZPSOLZEANG(:), ZPREC_FG(:), ZPREC_OB(:), ZPDPDT(:), &
& ZPDA(:), ZPVA(:), ZCA(:)
...
  IF(YDEXTRA_PRED%LMAP(YDEXTRA_PRED%CA))THEN
    ZCA=>YDEXTRA_PRED%VALUE(:,YDEXTRA_PRED%IMAP(YDEXTRA_PRED%CA))
    IF (ZCA(IPF) /= RMDI)THEN
      PRED(41,IPF) = ZCA(IPF)
    ELSE
      PRED(41,IPF) = 0.0_JPRB
    ENDIF
  ENDIF
...
```

Routine: arpifs/module/varbc_rad.F90

This routine contains a selection of predictors for diferent sensors and channels. A new selection of predictors is created for the subset of four all-sky IASI channels from this report. In this case, it is extended by the newly defined 41st predictor containing averaged cloud effect variable.

Changes made to this routine:

```
...
DO I = 1, SIZE(IASICHAN)
  IC = IASICHAN(I)
```

```
  SELECT CASE (IC)
    CASE (2951,2958,3049,3105)
      YCONFIG(INST_ID_IASI, IC)%NPARAM = 7
      YCONFIG(INST_ID_IASI, IC)%NPREDCS(1:7) = (/0,1,2,8,9,10,41/)
...
```

Routine: arpifs/op_obs/hop.F90

Passing the new predictor to minimization procedure requires it's initialization from the ODB values. ROBODY%BODY%FC_SENS_OBS was used to temporary store the averaged cloud effect parameter. This shows that extention of ODB tables will be required in the future.

Changes made to this routine:

```
...
IF( ANY(VARNOS_TO_PROCESS(:,:) == VARNO%RAWBT) ) THEN

    CALL YLVARBC_EXTRA_PRED%SETUP(YDGP5%NDLEN,(/YLVARBC_EXTRA_PRED%NVANG,YLVARBC_EXTRA_P
    CALL HSATANG(SATHDR,YDGP5%NDLEN,YDSET%OBSTYPE,YDSET%GROUP,YLVARBC_EXTRA_PRED%VALUE(:
    DO JOBS = 1,YDGP5%NDLEN
      YLVARBC_EXTRA_PRED%VALUE(JOBS,2) = SATHDR%SAT%SOLAR_ZENITH(JOBS)
      YLVARBC_EXTRA_PRED%VALUE(JOBS,3) = ROBODY%BODY%FC_SENS_OBS(JOBS)
    ENDDO
...
```

Routine: arpifs/op_obs/hretr_rad.F90

In this routine we call for a setup of extra predictors, including the averaged cloud effect. Since VARBC predictors are initialized at the begining of the routine, before averaged cloud effect is calculated, it's initialized with zeros so it won't affect initial bias calculation for all channels. Later, ROBODY%BODY%FC_SENS_OBS is filled with averaged cloud effect values and the bias is then recalculated for all-sky IASI channels.

Changes made to this routine:

```
...
ZCA(JOBS)         = 0.0_JPRB
ROBODY%BODY%FC_SENS_OBS(JOBS)=ZCA(JOBS)
...
! Set up and fill special VarBC predictors

CALL YLVARBC_EXTRA_PRED%SETUP(YDGP5%NDLEN,(/YLVARBC_EXTRA_PRED%NVANG, &
& YLVARBC_EXTRA_PRED%SOLZEANG,YLVARBC_EXTRA_PRED%CA/))
YLVARBC_EXTRA_PRED%VALUE(:,1)=ZNVANG
YLVARBC_EXTRA_PRED%VALUE(:,2)=ZSOLZENANG
YLVARBC_EXTRA_PRED%VALUE(:,3)=ZCA
CALL YDVARBC%PREDICTORS(YDGP5, IDATOB, ITIMOB, ZLAT, ZLON, ZXPRED, &
& YLVARBC_EXTRA_PRED, LD_MWAVE=.FALSE.)
```

```
CALL YDVARBC%BIAS (IXVARBC, IMXBDY, ICMBDY, YDGP5%NDLEN, ZXPRED, &
& ZBIAS_PREVIEW, ZBODYPRED)
...
ROBODY%BODY%FC_SENS_OBS(IBODY)=ZCLDA
...
IF(.NOT. LECMWF .AND. ISENSOR == INST_ID_IASI .AND. &
   & (SATGRP_TABLE(YDSET%GROUP)%CLD_RTCALC_ASSIM .OR. &
   & SATGRP_TABLE(YDSET%GROUP)%CLD_RTCALC_SCREEN)) THEN

   DO ILOOP=1,SIZE(SATOBERR_TABLE(YDSET%GROUP)%ICH_NUM)
     ICHAN=SATOBERR_TABLE(YDSET%GROUP)%ICH_NUM(ILOOP)

     DO IBODY=1,ROBODY%REPORT_END_ROW(YDGP5%NDLEN)
       JOBS = ROBODY%REPORT_NUMBER(IBODY)
       IF(ROBODY%BODY%VARNO(IBODY) == VARNO%RAWBT) THEN ! Radiance datum
         ZOBSV=ROBODY%BODY%OBSVALUE(IBODY)
         IF(ZOBSV /= RMDI) THEN
           IF (NINT(ROBODY%BODY%VERTCO_REFERENCE_1(IBODY))==ICHAN) THEN
             YLVARBC_EXTRA_PRED%VALUE(JOBS,3)=ROBODY%BODY%FC_SENS_OBS(IBODY)
           ENDIF
         ENDIF
       ENDIF
     ENDDO
     CALL YDVARBC%PREDICTORS(YDGP5, IDATOB, ITIMOB, ZLAT, ZLON, ZXPRED, &
     & YLVARBC_EXTRA_PRED, LD_MWAVE=.FALSE.)
     CALL YDVARBC%BIAS (IXVARBC, IMXBDY, ICMBDY, YDGP5%NDLEN, ZXPRED, &
     & ZBIAS_PREVIEW, ZBODYPRED)
     ICOUNT(:) = 0
     DO IBODY=1,ROBODY%REPORT_END_ROW(YDGP5%NDLEN)
       JOBS = ROBODY%REPORT_NUMBER(IBODY)
       JBODY = IBODY + 1 - ROBODY%REPORT_START_ROW(JOBS)
       IF(ROBODY%BODY%VARNO(IBODY) == VARNO%RAWBT) THEN
         ROBODY%BODY%BIASCORR(IBODY) = ZBIAS_PREVIEW(JOBS,ICOUNT(JOBS))
         ZOBSV=ROBODY%BODY%OBSVALUE(IBODY)
         IF(ZOBSV /= RMDI) THEN
           ICOUNT(JOBS)=ICOUNT(JOBS)+1
           IF (NINT(ROBODY%BODY%VERTCO_REFERENCE_1(IBODY))==ICHAN) THEN
             ZBIAS=ZBIAS_PREVIEW(JOBS,JBODY)
             IF(ZBIAS /= RMDI) THEN
               IF(ZTBTOT(JOBS,ICOUNT(JOBS)) /= RMDI) THEN
                 SATBODY%RADIANCE_BODY%CLD_FG_DEPAR(IBODY)=ZOBSV- &
                 & ZTBTOT(JOBS,ICOUNT(JOBS))-ZBIAS
               ENDIF
             ENDIF
           ENDIF
         ENDIF
       ENDIF
```

```
      ENDDO
    ENDDO
ENDIF
...
```

An assimilation cycle was initialized, using the averaged cloud effect variable as an extra VARBC predictor. Figure 11 shows that the extra predictor is initialized and enters the minimization step where it is updated.

```
ix=2544
pdate=20250115
class=rad
key=3 16 3105
label=Tb    metop    1     3 SENSOR=iasi    channel=3105
ndata=1101
npred=7
predcs=0 1 2 8 9 10 41
param0=-7.102E-02  4.354E-02 -2.650E-02 -1.179E-03  2.831E-02  1.028E-02  0.000E+00
params=-6.593E-02  3.987E-02 -2.363E-02  1.012E-02  2.570E-02  2.361E-02  5.156E-03
hstgrm=0 0 1 0 2 0 2 0 1 0 0 1 2 2 2 0 0 1 0 1 5 1 1 7 4 5 3 6 8 13 11 15 13 17 20 15
0 0 0 0 0 0 0 0 0 0 0 0 0 0 1 0 0
predxcnt=0 0 0 0 0 0 0 0 0 0 0 0 0 0 0 0 0 0 0 0 0 0 0 0 0 0 0 0 0 0 0 0 0 0 0 0 0 0
predmean=-2.147E+09 -2.147E+09 -2.147E+09 -2.147E+09 -2.147E+09 -2.147E+09 -2.147E+09
predxcov= 0.000E+00 -2.147E+09 -2.147E+09 -2.147E+09 -2.147E+09 -2.147E+09 -2.147E+09
09 -2.147E+09 -2.147E+09 -2.147E+09 -2.147E+09 -2.147E+09 -2.147E+09  0.000E+00 -2.14
147E+09 -2.147E+09 -2.147E+09 -2.147E+09  0.000E+00 -2.147E+09 -2.147E+09 -2.147E+09
```

Figure 11: VARBC output for IASI channel 3105, containing new predictor (41)

Further tests showed high sensitivity to the selection of different all-sky components, resulting in a crash during the data assimilation cycle. Further tests are needed in order to asses the source of said sensitivity and what further changes need to be made in order to properly apply a cloud-dependant VARBC predictor.

9 Conclusion

This study shows that all-sky assimilation of infrared radiances using the Okamoto methodology for observation error modeling can improve the model background state when appropriate quality control is applied. Rejection of strongly cloud-affected and poorly simulated observations is essential to prevent spurious increments and degradation near the surface. Independent observations confirm improved representation of the upper atmosphere, while remaining residual biases highlight the need for further refinement. The introduction of a cloud-dependent VARBC predictor is a promising step toward a more consistent bias correction in all-sky conditions, although additional work is required to ensure robustness. Next steps would be to refine the usage of a cloud-dependent VARBC predictor and examine the impact on the forecast using the final refined configuration.

References

[1] Panežić, S., 2024: Data assimilation of all-sky radiance observations from MTG IRS

[2] Okamoto, K., T. Ishibashi, I. Okabe, 2023: All-sky infrared radiance assimilation of a geostationary satellite in the Japan Meteorological Agency's global system. Quarterly Journal of the Royal Meteorological Society,Quart. J. Roy. Meteor. Soc, 149, 2477-2503

[3] Neduncheran Adhithiyan (2025, April 1st) Data Assimilation Session: AllSky VIS/IR assimilation activities at GeoSphere Austria; 5th ACCORD ASW, Zalakaros

[4] Auligné, T., McNally, A. P., Dee, D. P., 2007: Adaptive bias correction for satellite data in a numerical weather prediction system. Quarterly Journal of the Royal Meteorological Society, 133(624), 631–642.